Chapter 5

Brassica nigra derived catalyst for biodiesel synthesis

5.1 Introduction

This study depicts the *Brassica nigra* derived heterogeneous base catalyst in the transesterification of edible and non-edible oil for biodiesel synthesis. *Brassica nigra* (mustard) plant of the family Brassicaceae is cultivated in central Africa, Caspian steppes, southern Russia and throughout India, and is the oldest recorded species dating back to 5000 years [272]. It is cultivated for its seed oil which is used for various purposes particularly in cooking. The tender leaf of immature plants is consumed as vegetables and salad. *B. nigra* plant, seed as well as the extracted oil have a unique position in folk medicine. The oil is used in the treatment of common cold with mucus [273], and the plant is a remedy for arthritis, skin diseases, rheumatism, foot ache and lumbago [272,274]. The plant is reported for antimicrobial [275], anti-hyperglycaemic and anti-nociceptive properties [273]. It has also been reported that *B. nigra* is used in the treatment of various non-communicable diseases like diabetes, cardiovascular diseases, neurological disorders, respiratory diseases, joint diseases, cancer, vitiligo, etc. [276].

Waste *B. nigra*, obtained after harvesting oil seeds, is also used in the preparation of *Khar* by the Bodo peoples of Assam of North-East India. The water extract of *B. nigra* ash (*Khardwi*) is also found to be highly alkaline. In this context, it was assumed that the highly basic nature of the ash of *B. nigra* plant could be employed as an efficient heterogeneous catalyst in the transesterification reaction of oil to produce biodiesel. The literature study confirms that *B. nigra* agro-waste is available globally and no one has reported its chemical composition and catalytic activity in the production of biodiesel, and for any other reactions also. Hence, we are motivated to investigate the catalytic activity for base-catalysed biodiesel synthesis reaction using *B. nigra* derived ash as a base catalyst. The application of this waste plant as the heterogeneous base catalyst for the synthesis of biodiesel will add another dimension in discovering sustainable raw materials which is renewable and environmentally benign. In the present study, the potential of waste *B. nigra* plant has been examined as the heterogeneous catalyst for the synthesis of biodiesel using edible and non-edible oils. The effects of catalyst loading, MTOR, reaction temperature, activation energy, reusability and leaching of the catalyst were investigated along with the comparison study with reported agricultural waste derived catalysts. This waste plant derived material as the catalyst showed excellent catalytic activity, and thus, it has great potential for biodiesel synthesis that will help to reduce biodiesel cost. To the best of our knowledge, this would be the first report for the utilization of agricultural waste plant derived *B. nigra* ash as a catalyst for the synthesis of biodiesel.

5.2 Materials and methods

5.2.1 Materials

The waste *B. nigra* plant obtained after harvesting the seeds was collected from the Goybari village of Dotma under Kokrajhar district, Assam, India for the preparation of catalyst. To investigate the catalytic activity of the prepared catalyst, soybean oil was purchased in the market of Kokrajhar, Assam, India. The catalytic activity of the catalyst was also tested with non-edible oils *viz*. Jatropha oil obtained from LIFERR^{TM} Naturally Elite, India, and *Thevetia peruviana* oil which is extracted with hexane from the seeds collected from Kokrajhar, India [11]. The chemicals used in this study are mentioned in **Chapter 2** (**Section 2.2.1**, **Page no. 27**).

5.2.2 Methods

5.2.2.1 Preparation of catalyst

B. nigra plants along with seeds were gathered from the field where it was cultivated and allowed to dry under sun for 15 days. After untying the seeds from the plants, a similar procedure as mentioned in **Chapter 3 (Section 3.2.2.1, Page no. 71)** was employed for the preparation of catalyst.

5.2.2.2 Catalyst characterization

Similar procedure was followed for XRD, BET, XPS, TEM and pH analyses as mentioned in **Chapter 2 (Section 2.2.2.2, Page no. 28–29)**. FT-IR, AAS and SEM-EDX analyses are done as per the procedure mentioned in **Chapter 4 (Section 4.2.2.2, Page no. 111)**.

5.2.2.3 Biodiesel synthesis and characterization

The biodiesel synthesis was performed by reacting the soybean oil with methanol using the calcined *B. nigra* catalyst in a 100 mL round bottomed flask fitted with a hot-plate magnetic stirrer at room temperature (32°C), 45°C, 55°C and 65°C. Non-edible *Jatropha curcas* oil and *Thevetia peruviana* oil was also utilized in the synthesis of biodiesel. The optimization of reaction conditions was carried out as per the procedure mentioned in **Chapter 2 (Section 2.2.2.3, Page no. 29)**. Progress of rection and extraction of biodiesel were performed as per the procedure mentioned in **Chapter 4 (Section 4.2.2.3, Page no. 112)**. Characterizations of oil and the produced biodiesel by FT-IR, FT-NMR and GC-MS were performed as mentioned in **Chapter 4 (Section 4.2.2.3, Page no. 112)**. The properties of the produced biodiesel were determined as per the procedure mentioned in **Chapter 2 (Section 2.2.2.3, Page no. 30)**.

5.2.2.4 Determination of activation energy and pre-exponential factor

The method described in **Chapter 2 (Section 2.2.2.4, Page no. 30)** was followed for the determination of activation energy and pre-exponential factor.

5.3 Results and discussion

5.3.1 *Brassica nigra* catalyst characterization

5.3.1.1 XRD analysis

The XRD pattern of calcined *B. nigra* catalyst is depicted in **Fig. 5.1**. The XRD peaks were analysed by comparing the different 2θ values with Joint Committee on Powder Diffraction Standard (JCPDS) data as well as with reported literatures. The analysis revealed the presence of mixtures of inorganic components. The study showed the potassium as one of the major components in the catalyst which was found in the form of K_2CO_3, K_2O and KCl. The JCPDS data comparison with the XRD pattern indicated that the high intense peaks at 2θ values of 28.29 and 40.52 and other peaks at 50.15, 58.81, 66.36 and 73.8 are due to KCl indicating high percentage of K in the catalyst. In a similar study, Vadery et al. [100] reported the presence of KCl in the coconut husk ash catalyst with comparable 2θ values. The presence of K_2O in the present catalyst was indicated by the peaks at 2θ values 27.80, 39.52, 46.70 and 48.12. Similarly, the peaks at 2θ values 26.78, 29.66, 31.04, 34.07 and 41.89 showed the existence of K_2CO_3 in the catalyst which is in accordance with JCPDS data and XRD results of *Musa balbisiana* peel catalyst reported by Gohain et al. [109]. This study revealed that the 2θ values at 32.32, 37.18, 53.90 and 66.60 are due to the CaO present in the catalyst. Similar 2θ values for CaO were also reported by Laskar et al. [213], Wilson et al. [277] and Zhao et al. [50] in their catalysts derived from snail shell, dolomitic rock and rice husk, respectively. Pathak et al. [108] also reported the presence of CaO in their catalyst obtained from *Musa acuminata* peel with comparable 2θ values. The XRD peak in the *B. nigra* catalyst at 2θ value of 21.38 is due to the presence of SiO_2 which is supported by the result of straw slag catalyst reported by Wang et al. [223]. Presence of Fe_2O_3 and $CaMg(CO_3)_2$ in the catalyst was revealed from the 2θ values at 33.25 and 45.07, respectively. The presence of dolomite, $CaMg(CO_3)_2$ in the present catalyst is supported with the 2θ value reported by Wilson et al. [277]. Li et al. [278] and Zeng et al. [217] also reported similar 2θ value for Fe_2O_3 in their studies. The XRD patterns reveals the presence of mixed crystalline components in the catalyst.

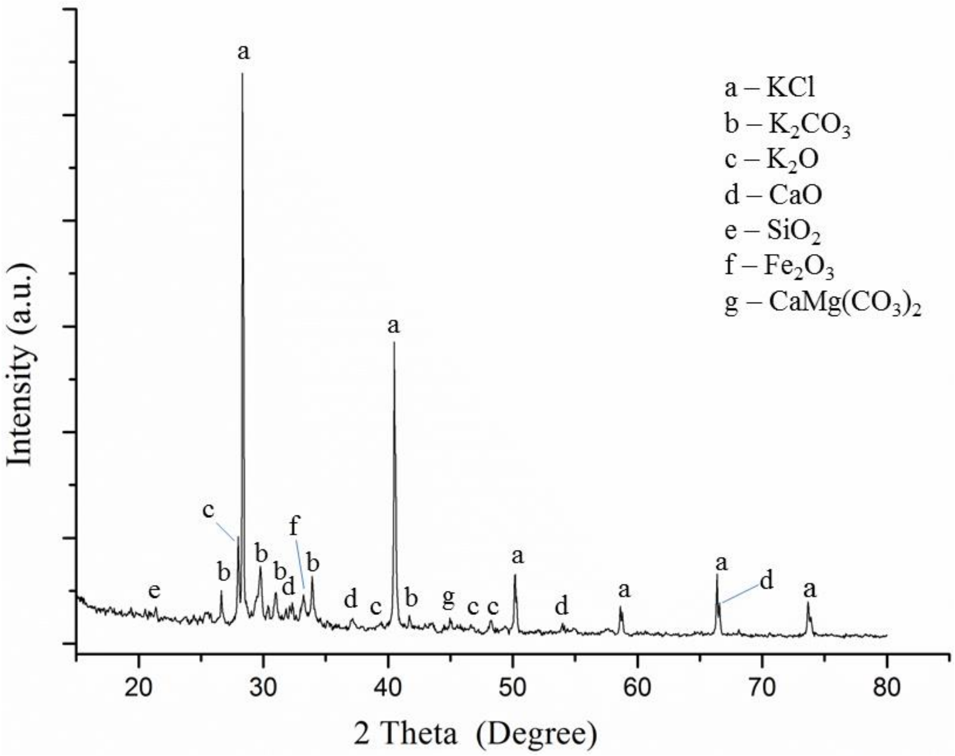

Fig. 5.1. XRD pattern of *Brassica nigra* catalyst calcined at 550 °C.

5.3.1.2 FT-IR analysis

The functional groups present in the calcined *B. nigra* catalyst were analysed by FT-IR (**Fig. 5.2**). The broad peak at 3148 cm^{-1} in the spectrum represents –OH group which is due to the adsorbed water molecules on the surface of the catalyst [107,115,279]. The peaks at 1461 cm^{-1} and 1392 cm^{-1} are due to C-O stretching frequencies indicating the presence of carbonate in the form of K_2CO_3 in the catalyst. Similar type of IR bands for carbonates were also reported for the ash catalysts in the works of Gohain et al. [109], Betiku et al. [105], Betiku et al. [115] and Mendonça et al. [12]. The C-O bending frequency of carbonate in the catalyst is represented by the peak at 1122 cm^{-1} which is in well agreement with the reported results of Betiku et al. [105], Betiku et al. [115] and Gohain et al. [109]. Si-O-Si stretching band of the SiO_2 present in the catalyst showed peak at 1030 cm^{-1} which conforms the results of Betiku et al. [105], Etim et al. [107], Chen et al. [229] and Zhao et al. [50] and this further supports the XRD peak of SiO_2 component (**Fig. 5.1**). The peak at 668 cm^{-1} attributes to OH bending vibration of water molecules adsorbed on the catalyst [105]. The IR peak at 624 cm^{-1} is signifying the stretching vibrations of Ca-O and K-O bonds that may be because of the presence of CaO and K_2O in the *B. nigra* catalyst which was also anticipated in the powder XRD study (**Fig. 5.1**). Therefore, the predictions concurred in the FT-IR study of *B. nigra* ash catalyst is consistent with the XRD analysis and confirms the presence of carbonate and oxide of metals in the catalyst.

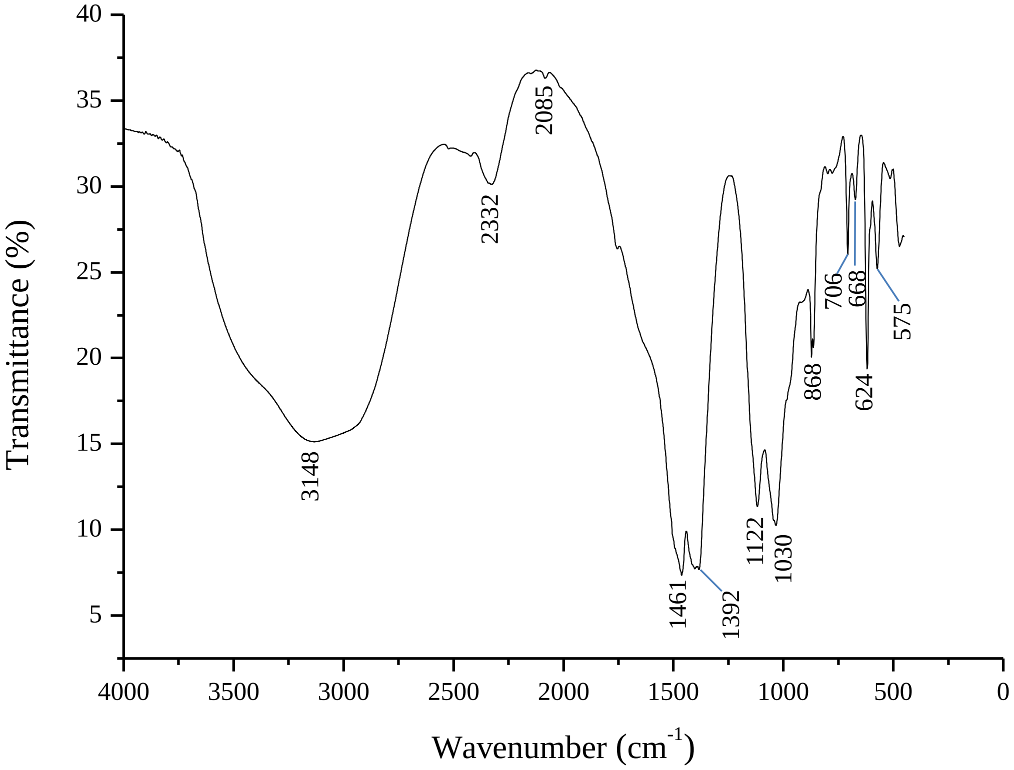

Fig. 5.2. FT-IR spectrum of *B. nigra* catalyst calcined at 550 °C.

5.3.1.3 Surface area, pore size and pore volume analysis

The BET surface area of the calcined *B. nigra* catalyst was found to be 7.308 $m^2\ g^{-1}$ and the resulted BJH pore volume was 0.011 $cm^3\ g^{-1}$. The characteristic of the N_2 adsorption-desorption isotherm of the catalyst is in conformity to the type-I isotherm (**Fig. 5.3**) representing the calcined *B. nigra* catalyst as microporous materials. However, Pathak et al. [108] and Laskar et al. [213] reported their biomass derived catalysts as the mesoporous materials which were represented with N_2 adsorption-desorption isotherm. The pore size distribution of the catalyst is from 1.25 nm to 2.05 nm (**Fig. 5.4**) and its pore diameter obtained is 1.67 nm which is further indicating microporous materials. Deka and Basumatary [11] in their study reported the surface area of *Musa balbisiana* catalyst as 1.487 m^2 g^{-1} which is lower compared to the present catalyst (7.308 m^2 g^{-1}). Similarly, Wang et al. [223] reported the surface area of gasified straw slag catalyst as 1.266 m^2 g^{-1} and Odude et al. [106] reported the surface area of banana peel catalyst as 4.442 m^2 g^{-1}. Sharma et al. [136] also studied the catalytic activity of the wood ash of *Acacia nilotica* in biodiesel production by calcination of ash catalyst at various temperatures and they reported the BET surface area ranging from 1.33 to 3.72 m^2 g^{-1}. They also reported that variation of calcination temperatures and time results in different surface areas of the catalyst. Very recently, Pathak et al. [108] also reported heterogeneous catalyst derived from *Musa acuminata* peel with much lower surface area (1.4546 m^2 g^{-1}) than the current catalyst reported herein. All these reported catalysts showed lower catalytic activity which is probably due to the lower surface area than the present catalyst derived from the waste *B. nigra* plant. The BET surface area of the catalyst has direct influence on the catalytic activity of the heterogeneous catalyst [136] and it has been reported that with increase in the surface area the catalytic activity increases [115].

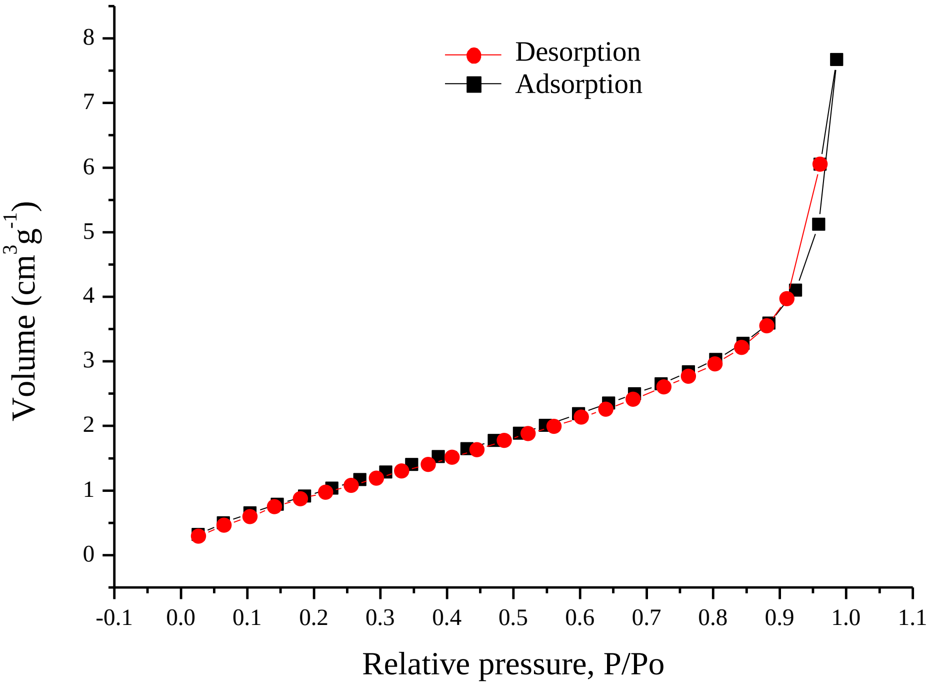

Fig. 5.3. N_2 adsorption-desorption isotherm of calcined *B. nigra* catalyst.

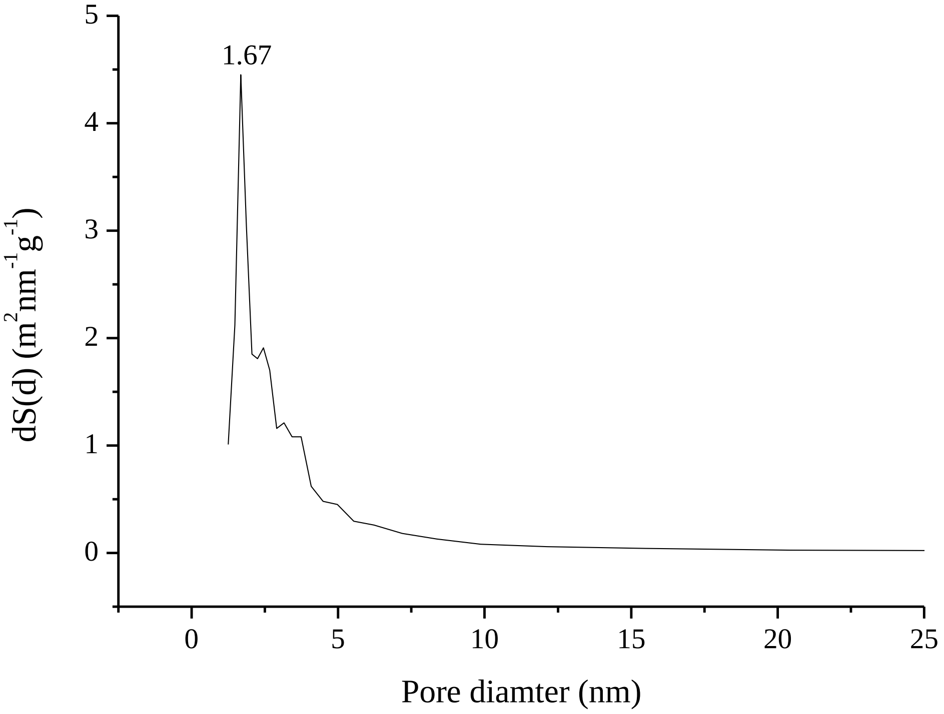

Fig. 5.4. Adsorption pore size distribution of calcined *B. nigra* catalyst.

5.3.1.4 SEM analysis

SEM was employed to study the morphological characters of the *B. nigra* catalyst. The SEM images depicted in **Fig. 5.5 A–C** are indicating the agglomeration of particles and also showing the clusters of various shape and size as well as layered like spongy fibrous microstructures that are produced on calcination. The bright particles observed in the SEM images may be due to the oxygenated matters in the catalyst which are probably the oxides of metals [113].

5.3.1.5 Analysis of elemental composition

The EDX (**Fig. 5.5 D**) study of the catalyst revealed the quantitative elemental composition of the catalyst and the results are presented in Table 1. The SEM-EDX study showed the highest percentage of K (56.13 wt.%) which is the dominant metal followed by Ca (26.04 wt.%). However, Na, Mg, Si, Fe, Mn, Zn and Sr were detected as minor components. AAS analysis of the calcined catalyst (**Table 5.1**) also depicted the highest amount of K (343.89 ppm) followed by Mg (238.95 ppm) and Ca (158.14 ppm) along with the low levels of Na, Mg, Fe, Mn and Zn. As shown by EDX and AAS studies, the high concentration of K in the *B. nigra* catalyst accredit the high basicity and accordingly showed highly efficient catalytic activity in the production of biodiesel from soybean oil via transesterification reaction. Betiku et al. [115] reported that the catalyst with higher potassium content showed better catalytic activity. Similarly, Mendonça et al. 2019 [12] in their study reported that heterogeneous catalyst derived from waste biomass with a high percentage of alkaline element favors for the transesterification of oil to biodiesel. Gohain et al. [109] determined the elemental composition of *Musa balbisiana* peel catalyst by EDX analysis and reported a higher percentage of potassium compared to other elements with good catalytic activity. Pathak et al. [108] and Basumatary et al. [129] also reported that a higher concentration of K in the waste biomass-derived heterogeneous catalysts contribute good catalytic activity in biodiesel synthesis.

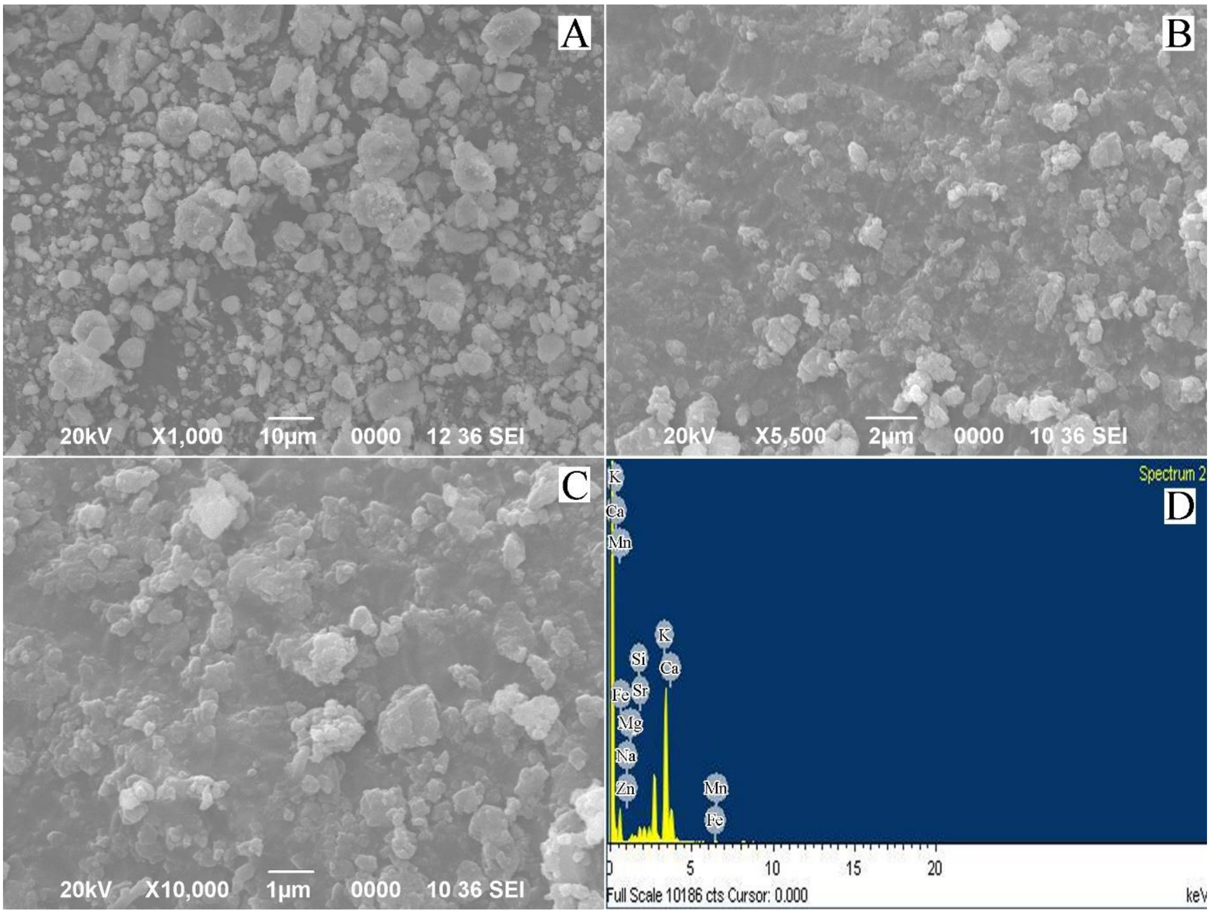

Fig. 5.5. SEM (A–C) and EDX (D) images of calcined *B. nigra* catalyst.

Further, the surface chemical composition of the calcined *B. nigra* catalyst as well as that of the 3rd recycled catalyst was determined by using XPS and the spectra are shown in **Fig. 5.6** and **Fig. 5.7**, respectively. The XPS analysis of the catalyst (**Table 5.2**) showed the presence of O (41.26%), C (29.91%), K (15.13%), Cl (4.32%), Ca (4.03%), Si (3.02%), Mg (0.85%), Fe (0.41%), Mn (0.37%), Na (0.29%), Sr (0.25%) and Zn (0.15%). Potassium was found to be the dominant component among the metals detected which is in well-agreement with XRD, EDX and AAS analyses. **Fig. 5.6** B depicts the high resolution XPS spectrum of O 1s showing the elemental oxygen as oxides in the catalyst with the binding energy of 530.99 eV. The two peaks in the spectrum of C 1s (**Fig. 5.6 C**) at 284.09 eV and 288.08 eV represent the binding energies of carbon (sp^2 hybridization) of carbonates present in the catalyst [108]. Potassium in the form of oxides and carbonates [108] in the catalyst showed binding energies of 292.11 eV and 294.59 eV in the high-resolution spectrum of K 2p (**Fig. 5.6 D**). The two peaks with binding energies of 345.90 eV and 349.37 eV in the spectrum of Ca 2p (**Fig. 5.6 E**) may be because of carbonate or oxide of calcium present in the catalyst [50]. The peak at a binding energy of 197.70 eV (**Fig. 5.6 F**) indicated chlorine due to the potassium chloride present in the catalyst which was also supported by the powder XRD analysis (**Fig. 5.1**). Thus, the elemental analysis reveals the presence of higher quantity of potassium as oxide, carbonate and chloride in the catalyst which might play as a key role in the catalytic activity for biodiesel production.

Table 5.1: Elemental composition of calcined *B. nigra* catalyst

Element	**SEM-EDX analysis of calcined catalyst**		**AAS analysis**	
	Weight (%)	**Atomic (%)**	**Concentration (ppm), calcined catalyst**	**Concentration (ppm), 3rd recycled catalyst**
Na	0.94	1.60	11.96	10.19
Mg	2.86	4.62	238.95	235.01
Si	5.37	7.50	nd[a]	nd[a]
K	56.13	56.33	343.89	320.93
Ca	26.04	25.49	158.14	151.21
Mn	0.05	0.03	6.04	8.38
Fe	1.26	0.89	19.49	21.44
Zn	1.63	0.98	4.19	5.47
Sr	5.72	2.56	nd[a]	nd[a]

[a]nd, Not determined.

Table 5.2: XPS analysis of surface composition of the *B. nigra* catalyst

Elements	**Calcined catalyst**	**3rd recycled catalyst**
	Atomic (%)	**Atomic (%)**
C1s	29.91	27.71
O1s	41.26	38.81
Na1s	0.29	0.63
Mg1s	0.85	3.24
Si2p	3.02	7.92
K2p	15.13	10.19
Ca2p	4.03	9.13
Mn2p1	0.28	0.23
Mn2p3	0.09	0.07
Fe2p1	0.31	0.29
Fe2p3	0.11	0.23
Zn2p1	0.08	0.35
Zn2p3	0.07	0.06
Sr3d	0.25	0.76
Cl2p	4.32	0.38

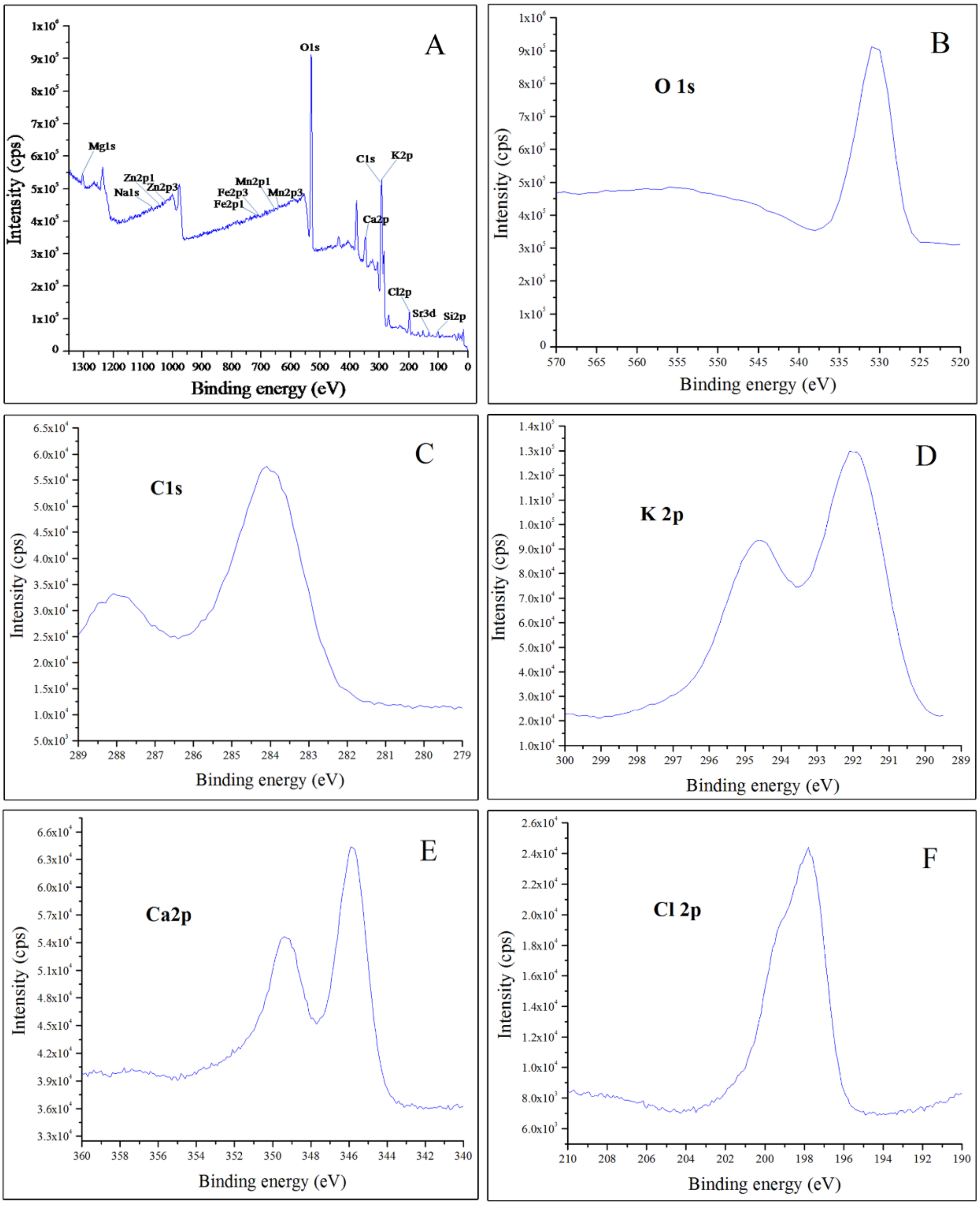

Fig. 5.6. (A) XPS survey spectrum of calcined *B. nigra* catalyst; XPS spectra of (B) O 1s, (C) C 1s, (D) K 2p, (E) Ca 2p and (F) Cl 2p.

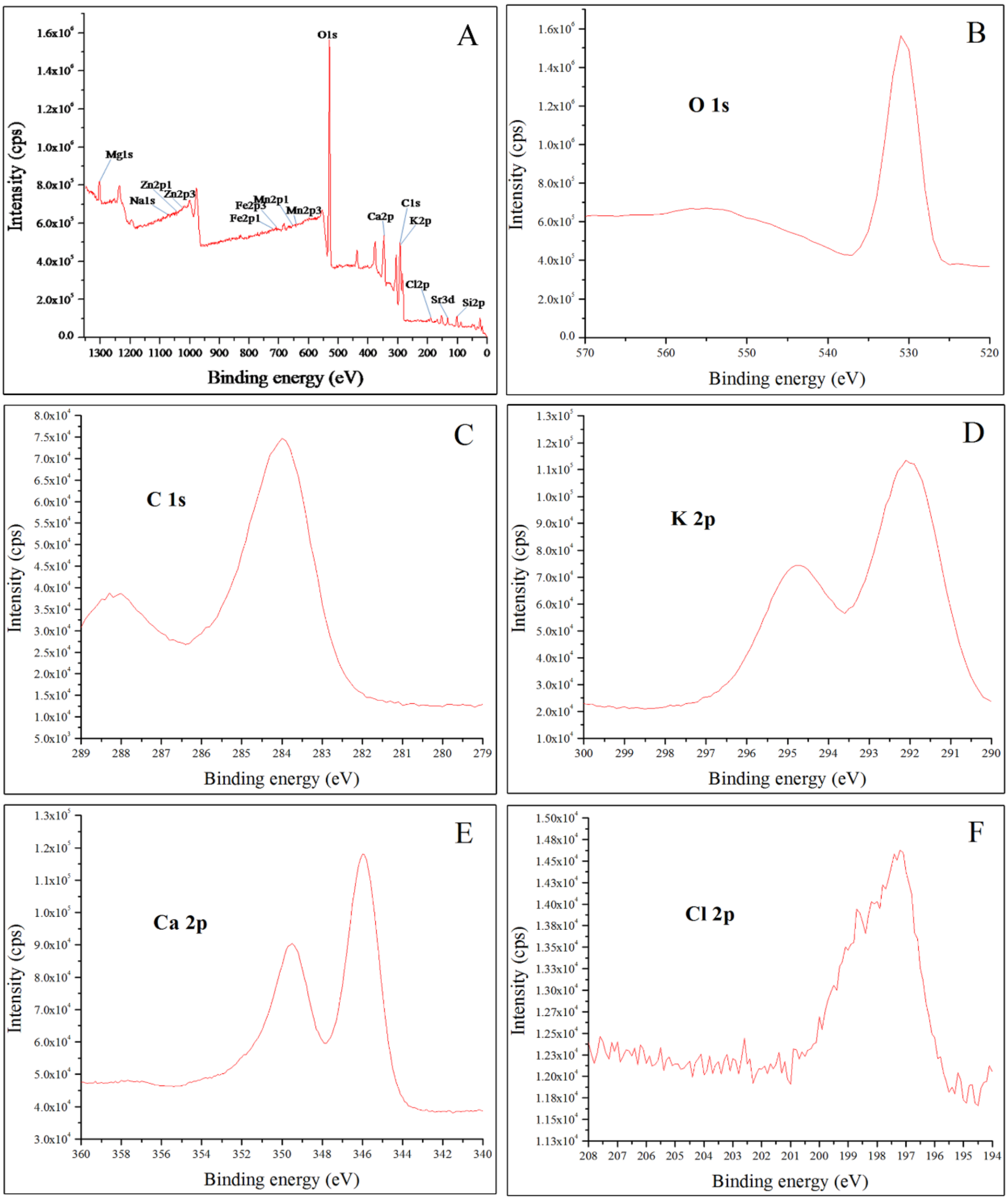

Fig. 5.7. (A) XPS survey spectrum of recycled catalyst (3rd cycle); XPS spectra of (B) O 1s, (C) C 1s, (D) K 2p, (E) Ca 2p and (F) Cl 2p.

5.3.1.6 TEM analysis

The TEM images shown in the **Fig. 5.8** illustrate the structural information of the calcined catalyst. The low magnification TEM images (**Fig. 5.8 A–C**) are indicating that the particles are of irregular size and shape with hexagonal, cylindrical and spherical. The smaller particles are may be oxides of metals and large particles may be the crystallite [223].

The smaller clusters of nano-size particles give effective surface area for the efficient catalytic activity [110,111]. In this study, presence of mixed polycrystalline nature of the catalyst is depicted from the SAED pattern (**Fig. 5.8 D**). Similarly, Talukdar and Deka [135] reported a heterogeneous catalyst derived from waste *Eichhornia crassipes* plant which is polycrystalline in nature.

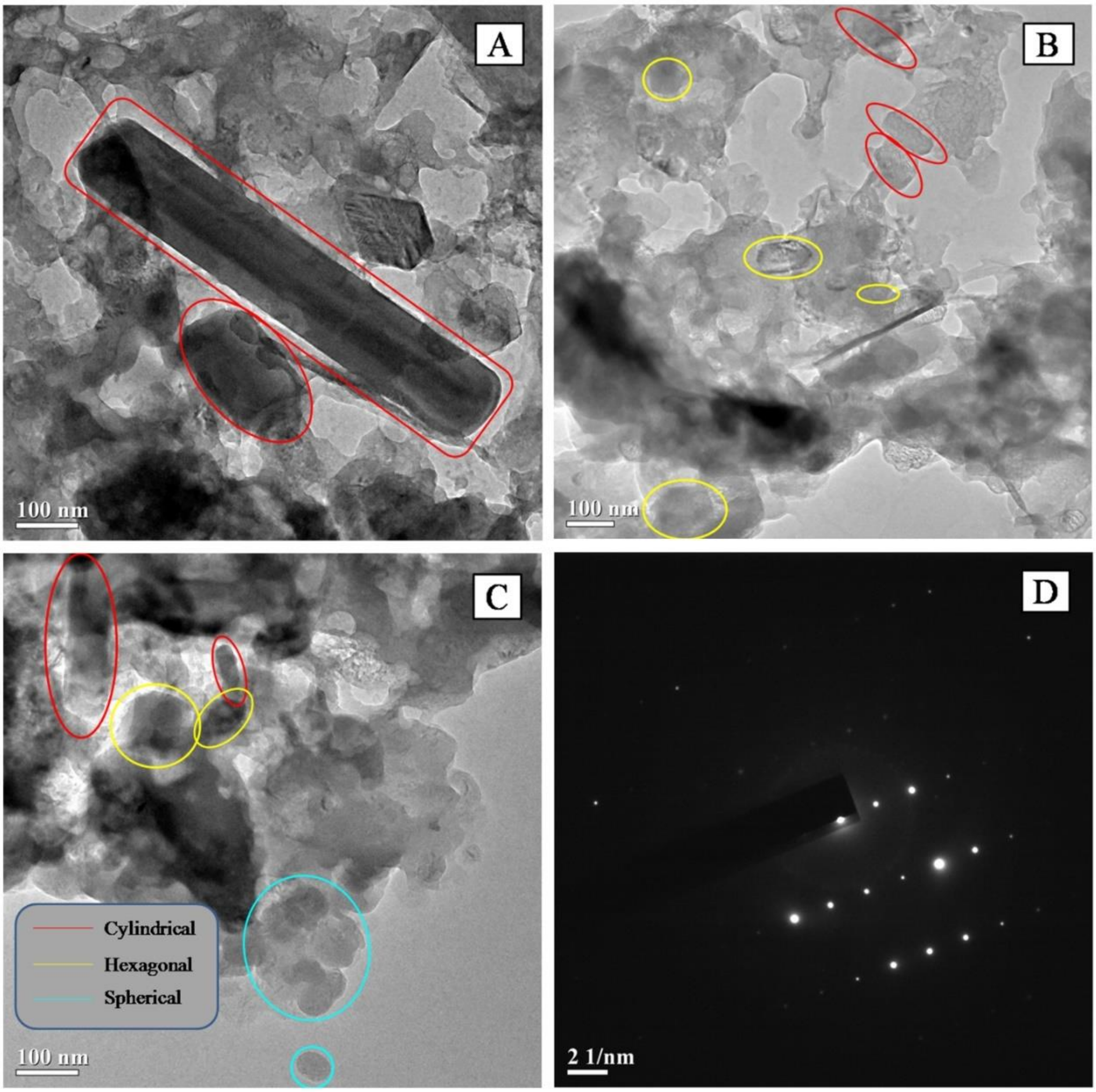

Fig. 5.8. TEM images (A–C) and SAED pattern (D) of calcined *B. nigra* catalyst.

5.3.1.7 pH measurement

The pH value of aqueous solution of calcined *B. nigra* catalyst was determined by dissolving 1 g of the calcined ash in different volume of water and the variation of pH value is shown in the **Fig. 5.9**. The catalyst showed a pH value of 11.91 (1 g in 5 mL water) which is representing the high basic nature of catalyst, and this pH value slightly decreases to 11.59 when 1 g of catalyst is dissolved in 30 mL of distilled water. As depicted by AAS, EDX and XPS analyses, the higher concentration of potassium in the catalyst is the key factor for its high basic character. However, waste *Eichhornia crassipes* plant derived heterogeneous base catalyst reported for organic transformation reaction by Talukdar and Deka [135] had a lower pH value of 9.6 (1 g in 20 mL water) compared to the current catalyst (pH = 11.76; 1 g in 20 mL).

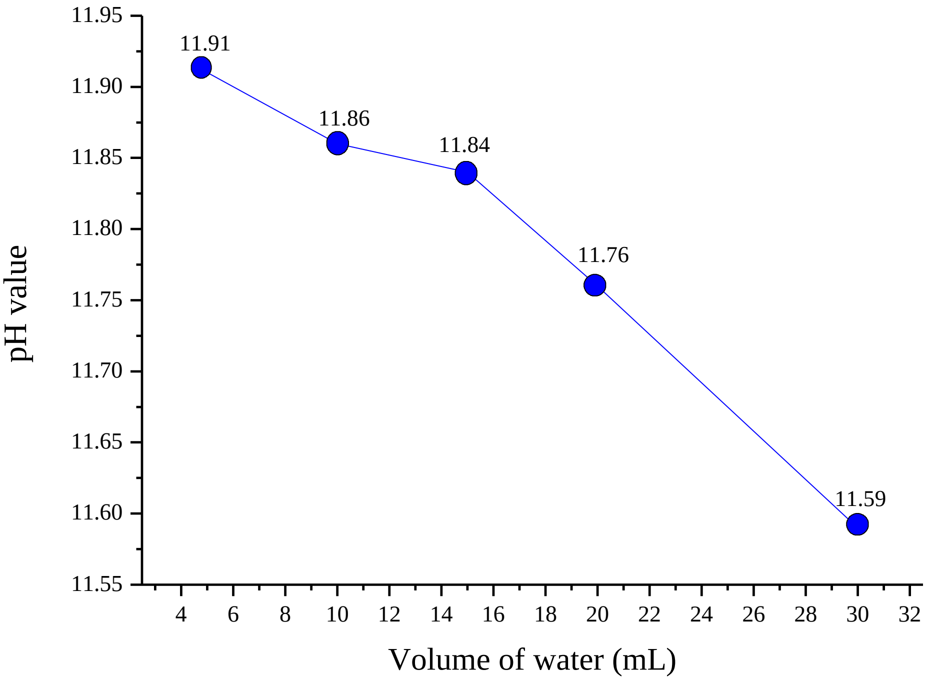

Fig. 5.9. Variation of pH value with volume of water dissolving 1 g of calcined *B. nigra* catalyst.

5.3.2 Catalytic activity study of *Brassica nigra* catalyst

5.3.2.1 Effect of catalyst load dosage

The amount of catalyst with respect to oil influences the rate of transesterification reaction. To examine the effect of catalyst loading on the yield of biodiesel and reaction time for conversion, various concentrations of the catalyst *viz*. 3 wt.%, 5 wt.%, 7 wt.% and 9 wt.% of oil were utilized for transesterification reaction of the soybean oil with methanol to oil ratio (MTOR) of 9:1 at ambient temperature (32 °C). The catalytic activity study (**Fig. 5.10**) depicts that the transesterification reaction with 7 wt.% of catalyst loading showed the superior result with 97.54% yield of biodiesel in a shorter reaction time of 85 min compared to the other catalyst loads. On increasing the loading of catalyst from 3 wt.% to 7 wt.%, the time taken for the reaction was found to decrease from 105 min to 85 min with a slight increase in the biodiesel yield from 93.86% to 97.54%, respectively. However, further increase in catalyst load to 9 wt.% under the same reaction conditions, no significant improvement of results in terms of the yield of biodiesel and reaction time were achieved. Thus, the optimum catalyst amount for the transesterification reaction was considered as 7 wt.%. In a similar study, Gohain et al. [109] reported that the biodiesel yield increased up to a certain level on increasing the catalyst amount and beyond the optimum catalyst concentration the yield of biodiesel remains almost the same.

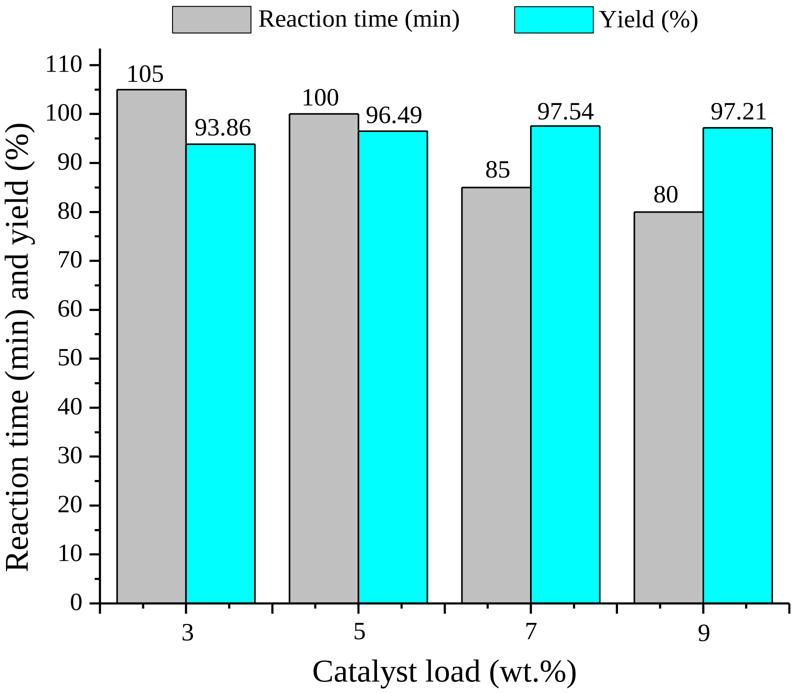

Fig. 5.10. Effect of catalyst loading (wt.%) on reaction time and biodiesel yield. Reaction condition: methanol to oil molar ratio = 9:1 and reaction temperature = 32°C.

5.3.2.2 Effect of methanol to oil ratio (MTOR)

As that of catalyst loading, MTOR also influences the rate of transesterification reaction for biodiesel synthesis. Using the optimum catalyst load of 7 wt.% and varying the MTOR such as 3:1, 6:1, 9:1, 12:1, 15:1 and 18:1, the biodiesel yield and reaction time taken were investigated at an ambient temperature (32°C), and the results are depicted in **Fig. 5.11**. It was observed that the reaction time for the transesterification reaction decreased with increasing MTOR from 3:1 (105 min) to 12:1 (75 min) along with the increase in the yield of biodiesel from 96% to 98.87%. Beyond MTOR of 12:1, no significant improvements in the reaction time and biodiesel yield were noticed, and this may be due to the disturbance of the active sites of the catalyst beyond optimum level of MTOR which leads to dilution of reaction mixture resulting in reduced interaction of oil and methanol with the catalyst in the transesterification reaction [135,230]. Thus, 12:1 MTOR was considered as the optimum level for biodiesel synthesis in the present study. Biodiesel synthesis by Sharma et al. [136], Vadery et al. [100], Wang et al. [223] and Uprety et al. [171] using various heterogeneous catalysts also indicated 12:1 as the optimum MTOR for the synthesis of biodiesel.

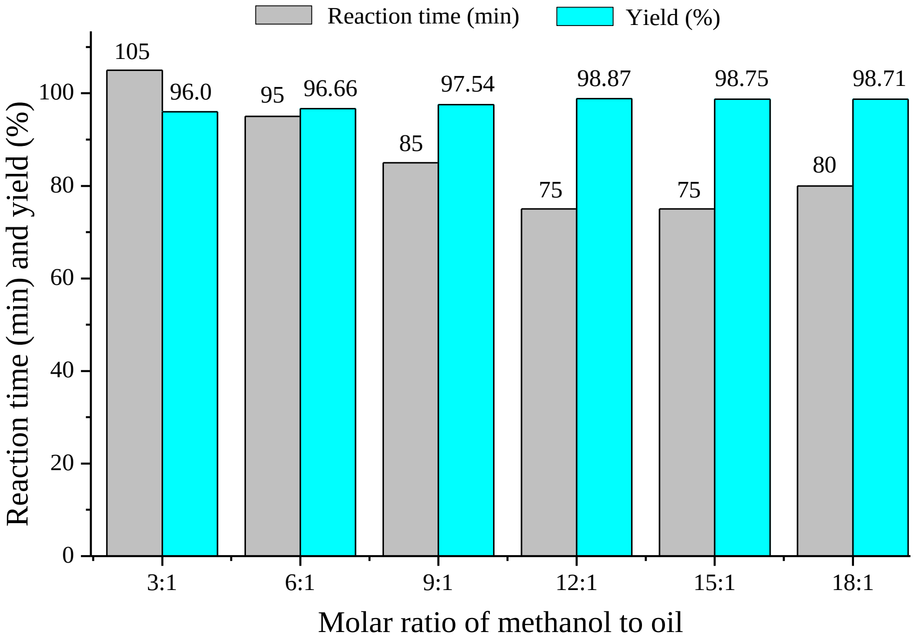

Fig. 5.11. Effect of methanol to oil molar ratio on reaction time and biodiesel yield. Reaction condition: catalyst loading = 7 wt.% and reaction temperature = 32°C.

5.3.2.3 Effect of reaction temperature

It is noteworthy to mention that the reaction temperature is also essentially a very important factor for biodiesel synthesis. Therefore, transesterification reaction was investigated at various temperatures *viz.* ambient temperature (32°C), 45°C, 55°C and 65°C under the ORCs of 12:1 MTOR and 7 wt.% catalyst loading, and the results are depicted in **Fig. 5.12**. It was observed that with increasing the reaction temperature, the reaction time decreased sharply from 75 min at 32°C (98.87% yield) to 25 min at 65°C (98.79% yield). Thus, it can be concluded that the calcined *B. nigra* catalyst has excellent catalytic activity in converting soybean oil to biodiesel with 98.79% yield in a short time period of 25 min under the ORCs of 12:1 MTOR, 7 wt.% of catalyst loading and reaction temperature of 65°C.

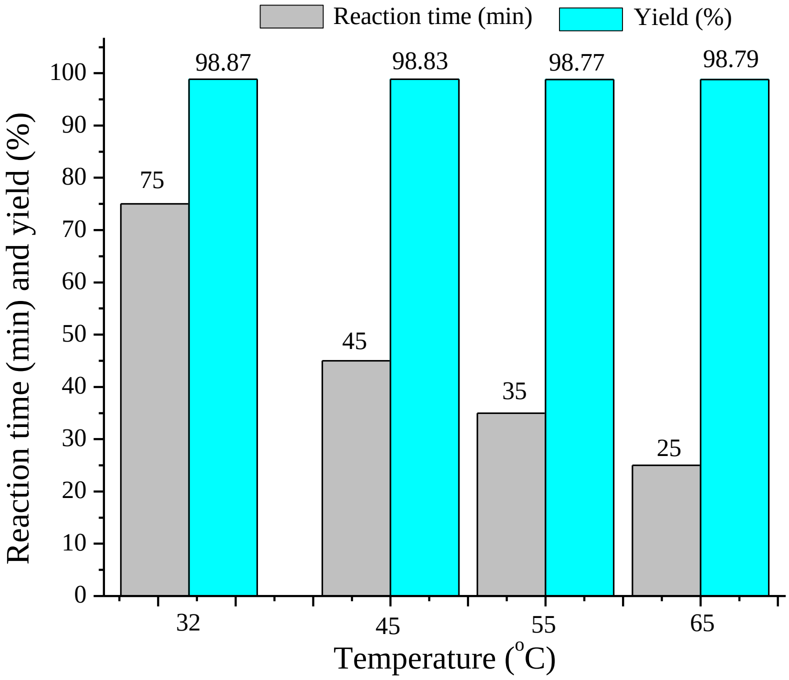

Fig. 5.12. Effect of temperature on reaction time and biodiesel yield. Reaction condition: catalyst loading = 7 wt.% and methanol to oil ratio= 12:1.

5.3.3 Comparison of *Brassica nigra* catalyst with other reported waste plant derived catalyst.

The study on the effects of MTOR, loading of catalyst and reaction temperature revealed that the ORCs for the transesterification reaction of soybean oil into biodiesel were 12:1 MTOR, 7 wt.% of catalyst and 65 °C reaction temperature which could produce biodiesel with 98.79% yield within a short reaction time of 25 min. Under the same reaction conditions, 98.87% biodiesel yield could be achieved within 75 min when the reaction was performed at an ambient temperature of 32 °C showing a very good catalytic activity even at the low reaction temperature. In this study, we also investigated the catalytic activity for biodiesel synthesis from non-edible oils such as Jatropha oil and *Thevetia peruviana* oil under the optimized reaction conditions. It showed similar trend of catalytic activities with the biodiesel yields of 98.26 and 97.78% from Jatropha and *Thevetia peruviana* oils within 30 and 25 min, respectively (**Table 5.3**, Entry 3 & 4). A comparative summary of the present catalyst with other reported heterogeneous base catalysts derived from waste plant/biomass is depicted in **Table 5.3**. As could be seen from **Table 5.3**, *B. nigra* derived catalyst showed better catalytic activity and this is due to its higher potassium content (56.33%) compared to other agricultural wastes derived catalysts such as *Musa balbisiana* underground stem (25.09%) reported by Sarma et al. [111], *Musa balbisiana* peels (41.37%) reported by Gohain et al. [109], *Lemna perpusilla* (11.32%) reported by Chouhan et al. [114], *Acacia nilotica* tree stem (5.7%) reported by Sharma et al. [136], etc. The explanation for high catalytic activity is also matching with the report of Betiku et al. [115] and Pathak et al. [108]. It can also be noticed from **Table 5.3** that the BET surface areas reported in the works of Mendonça et al. [12], Kaewdaeng et al. [280], Deka and Basumatary [11], Odude et al. [106], Pathak et al. [108], Wang et al. [223] and Kumar et al. [197] are smaller compared to that of *B. nigra* catalyst (7.308 m^2 g^{-1}), and this larger surface area might be one of the factors for the better catalytic activity in case of the present catalyst. Similarly, Uprety et al. [171] and Aslam et al. [110] also reported much longer reaction times for biodiesel synthesis using the catalyst derived from Birch bark and *Musa balbisiana* underground stem. Thus, superior and excellent catalytic activity of calcined *B. nigra* catalyst in terms of yield of biodiesel, reaction time and temperature amongst the heterogeneous catalysts summarized in **Table 5.3**, might be due to its higher potassium content (56.33 wt.%, **Table 5.1**) and hence showed highly basic nature of the catalyst (**Fig. 5.9**).

Table 5.3: Comparison of activity of the catalyst derived from waste *B. nigra* plant with reported heterogeneous base catalysts for biodiesel synthesis

Biodiesel feedstock	**Catalyst source**	**Surface area (m^2 g^{-1})**	**Parameter**				**Biodiesel, Y or C (%)**	**References**
			MTOR	**Catalyst (wt.%)**	**Temp (°C)**	**Time (min)**		
Soybean oil	*B. nigra*	7.308	12:1	7	65	25	98.79 (Y)	This work
Soybean oil	*B. nigra*	7.308	12:1	7	32	75	98.87 (Y)	This work
Jatropha oil	*B. nigra*	7.308	12:1	7	65	30	98.26 (Y)	This work
Thevetia peruviana oil	*B. nigra*	7.308	12:1	7	65	25	97.78 (Y)	This work
Soybean oil	Tucumã peels	1	15:1	1	80	240	97.3 (C)	[12]
Soybean oil	Snail shell	7	6:1	3	28	420	98 (Y)	[213]
Thevetia peruviana oil	*Musa balbisiana* trunk	1.487	20:1	20	32	180	96 (Y)	[11]
Mesua	*Musa*	38.71	9:1	5	275	60	95 (C)	[110]

ferrea oil	*balbisiana* underground stem							
Jatropha oil	*Musa balbisiana* underground stem	38.71	9:1	5	275	60	98 (Y)	[111]
Bauhinia monandra	Banana peel	4.442	7.6:1	2.75	65	69	98.5 (C)	[105]
Waste cooking oil	*Musa balbisiana* peel	10.176	6:1	2	60	180	100 (C)	[109]
Soybean oil	*Musa acuminata* peel	1.4546	6:1	0.7	32	240	98.95 (C)	[108]
Jatropha oil	*Lemna perpusilla*	9.622	9:1	5	65	300	89.43 (Y)	[114]
Rapeseed oil	Gasified straw slag	1.266	12:1	20	200	480	95 (C)	[223]
Palm oil	Birch bark	–	12:1	3	60	180	69.7 (C)	[171]
Jatropha oil	SrO-*Musa Balbisiana* underground stem	0.043	9:1	5	200	60	96 (Y)	[197]

MTOR–Methanol to oil ratio; Temp–Temperature; min–minute; Y–Yield; C–Conversion.

5.3.4 Reusability study of the *Brassica nigra* catalyst

As it is known that the reusability of catalyst in the subsequent reactions is one of the notable advantages and significant properties of the heterogeneous catalyst [12,229]. Accordingly, the reusability potential of the present catalyst was examined under the ORCs. The catalyst was separated from the reaction mixture under suction after completion of the reaction and washed with petroleum ether for several times followed by acetone. The regenerated catalyst was dried on a crucible under hot air oven at 110^{o}C for 4 h, kept in a desiccator and reused in the next cycle of reaction. Subsequently, a similar procedure was followed for every cycle of reaction. The results shown in **Fig. 5.13** indicate that the efficiency of the catalyst slightly decreases in each cycle of the reaction with the yield of biodiesel from 98.79% (fresh catalyst) to 96% (3rd cycle) along with increase in reaction time from 25 min (fresh catalyst) to 135 min (3rd cycle). In a similar study of heterogeneous catalyst derived from banana trunk, Deka and Basumatary [11] reported the decrease of biodiesel yield from 96% (1st run) to 91% (3rd run). Sarma et al. [111] reported 20% decrease in the activity of catalyst in the third consecutive reaction. Mendonça et al. [12] also reported the reusability of the catalyst obtained from *Astrocaryum aculeatum* up to 5th cycle of reaction with 17.3% decrease in activity. The decrease in the activity of the catalyst may be due to leaching or loss of active elements during subsequent transesterification reaction [109]. In addition, agglomeration of glycerol and methyl ester molecules may occur over the catalyst surface on repeated use of the catalyst which may block the active sites resulting in a reduced biodiesel yield [108].

To investigate the leaching of active components in the recycled catalyst, AAS (**Table 5.1**) and XPS (**Fig. 5.6; Table 5.2**) analyses were carried out. The AAS analysis of the 3rd recycled catalyst showed a decrease of K from 343.89 ppm (fresh catalyst) to 320.93 ppm (3rd cycle) along with the negligible decrease of Mg and Ca concentration (**Table 5.1**) which may be the factor for the decrease in efficiency of the present catalyst. Similarly, XPS analysis of the recycled catalyst confirmed the decrease of potassium content from 15.13% (fresh catalyst) to 10.19% (3rd cycle). In addition to potassium, the XPS study (**Table 5.2**) also showed the decrease in atomic percentage of carbon, oxygen and chlorine in the recycled catalyst indicating the probable leaching of K_2CO_3, K_2O and KCl. Thus, the leaching of K in the 3rd recycled catalyst confirmed the role of K in the reaction. However, the leaching of Ca concentration was not seen in the XPS analysis which further confirmed that K in the form of K_2CO_3 and K_2O is the main active component which played the major role for the efficient catalytic activity in the biodiesel synthesis studied herein. Thus, it is important to mention that the calcined *B. nigra* catalyst could be potentially reused for several cycles of reaction with no significant loss in the efficiency of the catalyst.

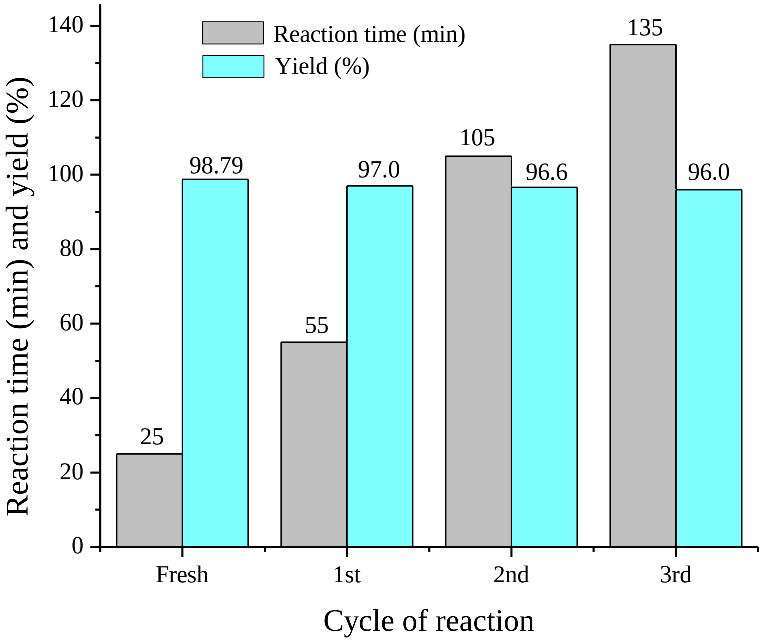

Fig. 5.13. Reusability of calcined *B. nigra* catalyst. Reaction conditions: catalyst loading = 7 wt.%, methanol to oil ratio= 12:1 and reaction temperature = 65°C.

5.3.5 Determination of activation energy and pre-exponential factor

In this study, the efficacy of calcined *B. nigra* catalyst in lowering the activation energy of the transesterification reaction was calculated from the slope (= E_a/R) of the Arrhenius plot drawn by plotting ln k values against the inverse of temperature. The rate constants at different temperatures were calculated from the data obtained from transesterification reactions and were found to be 0.06, 0.07, 0.10 and 0.18 min^{-1} at 32, 45, 55 and 65 °C respectively. The Arrhenius plot is drawn and is shown in **Fig. 5.14**. From the straight line (**Fig. 5.14**) obtained by linear fitting of the graph, the slope was found to be -3.3525 and accordingly the activation energy value was calculated to be 27.87 kJ mol^{-1}. This activation energy for transesterification of soybean oil with methanol using the calcined *B. nigra* catalyst is also well within the range of reported results (21 kJ mol^{-1} to 84 kJ mol^{-1}) for the synthesis of biodiesel via transesterification of oil [211,212,257,261]. The value of activation energy of the present catalyst is analogous with the *H. fragrans* and *S. indicum* catalysts described in Chapter 2 and Chapter 3, whereas lower than that of *M. champa* catalyst of Chapter 3. The activation energy (61.23 kJ mol^{-1}) reported by Mendonça et al. [12] for the transesterification of soybean oil using the heterogeneous catalyst derived from *Astrocaryum aculeatum* is comparatively higher to that of the present study. It was reported in the literatures that a diffusion and mass control reactions have activation energy of 10–15 kJ mol^{-1} and the activation energy greater than 25 kJ mol^{-1} truly favours the chemically controlled reactions, and thus the present catalyst with the activation energy of 27.87 kJ mol^{-1} supported that the transesterification reaction of oil is a chemically controlled reaction [212,281].

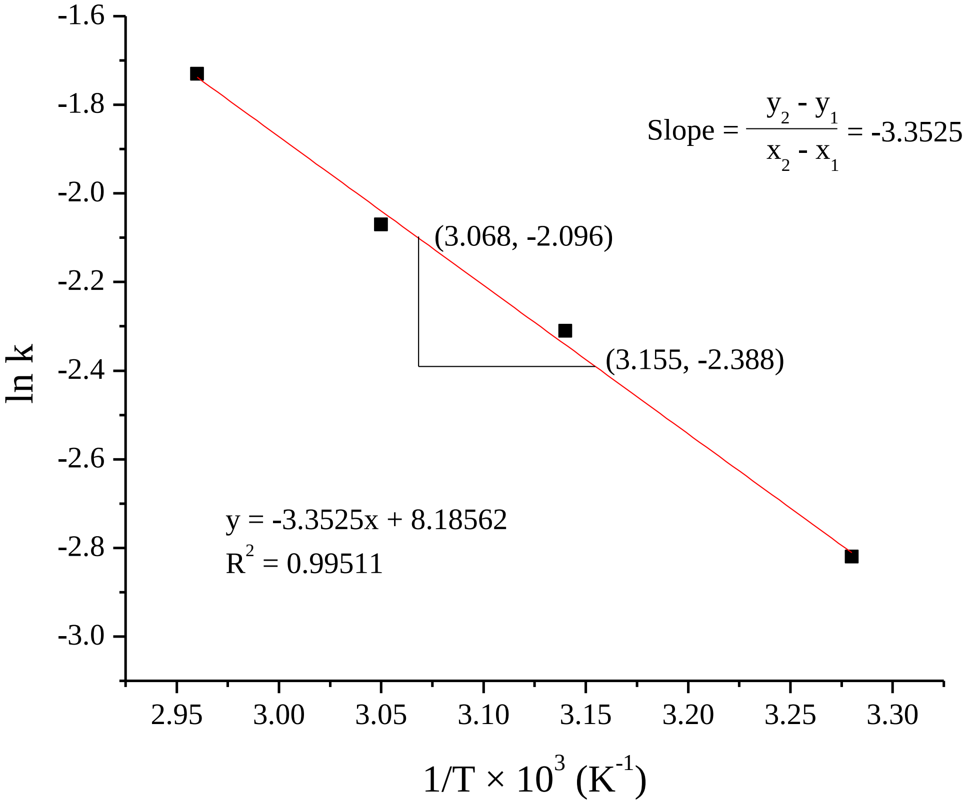

Fig. 5.14. Arrhenius plot of ln k vs 1/T for pseudo-first order kinetic reaction.

5.3.6 Characterization of soyabean oil biodiesel

5.3.6.1 FT-IR analysis

The absorption peak due C=O stretching vibration at 1744 cm^{-1} due to glyceride linkage in soybean oil (**Fig. 5.15**) changes to 1742 cm^{-1} due to the methyl esters in biodiesel (**Fig. 5.15**) representing the conversion in the transesterification reaction. The peaks due to -CH=CH- stretching frequencies present in both the oil and biodiesel are observed at 3008 cm^{-1} and 3009 cm^{-1} respectively. The signals at 2928 cm^{-1} and 2854 cm^{-1} in the oil and the signals at 2926 cm^{-1} and 2855 cm^{-1} in biodiesel are due to C-H stretching vibrations. The CH_3 bending vibrations in the case of oil are observed at 1459 and 1374 cm^{-1}, and that of biodiesel is seen at 1466, 1437 and 1362 cm^{-1}. The IR peaks at 1240, 1160 and 1096 cm^{-1} in the oil, and the IR peaks at 1247, 1195 and 1170 cm^{-1} in the biodiesel represent the C-O stretching bands of triglyceride and ester molecules, respectively. The –CH_2– rocking of the fatty acid chains showed IR signal at 720 cm^{-1} in case of oil and 724 cm^{-1} in the case of methyl ester molecules.

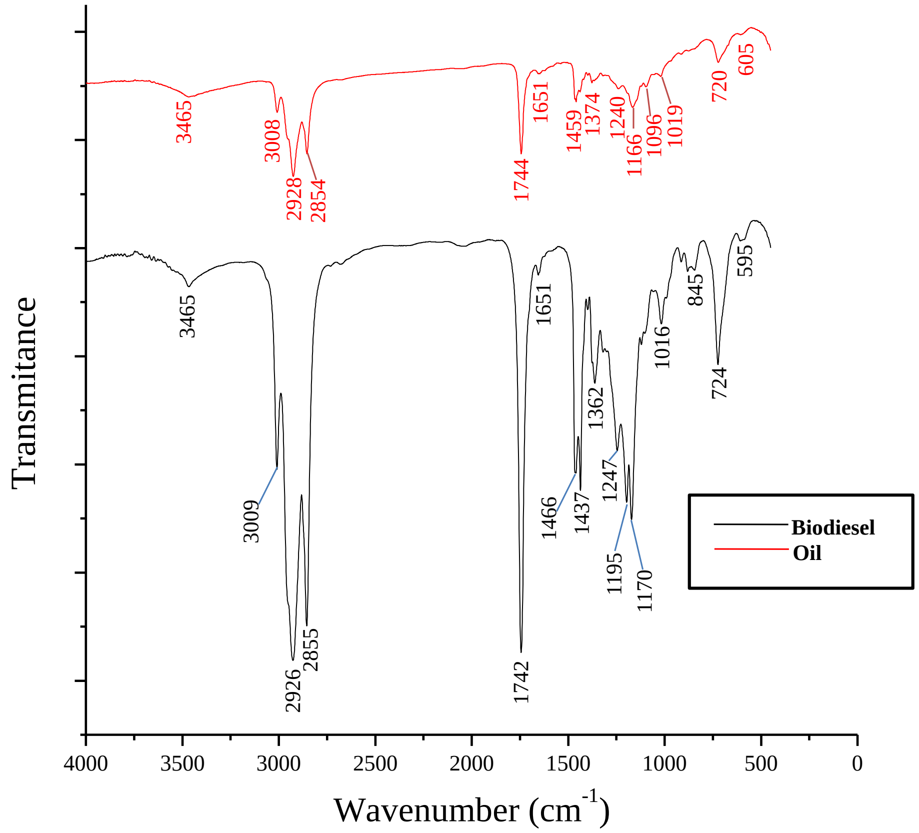

Fig. 5.15. FT-IR spectra of soybean oil and biodiesel.

5.3.6.2 NMR analysis

The spectral analysis of the soybean oil and biodiesel by ^{1}H NMR (**Fig. 5.16** and **Fig. 5.17**) and ^{13}C NMR (**Fig. 5.18** and **Fig. 5.19**) showed the major differences in signals which clearly indicated the conversion of oil to biodiesel. The signals representing the glycerol moiety of glyceride in the oil at δ 4.115–4.160 ppm (dd, ^3J = 6, 12 Hz) and δ 4.283–4.323 ppm (dd, ^3J = 4, 12 Hz) (**Fig. 5.16**) disappeared in the biodiesel spectrum (**Fig. 5.17**) and the appearance of a new signal at δ 3.648 ppm in the biodiesel spectrum due to the methoxy proton (-CO-OC$\boldsymbol{H}_3$) clearly showed the conversion of oil to biodiesel. Similarly, the signals at δ 61.99 ppm and δ 68.839 ppm in the ^{13}C NMR spectrum of soybean oil (**Fig. 5.18**) due to the methine and methylene carbons of the glycerine moiety are disappeared in the ^{13}C NMR spectrum of FAME (**Fig. 5.19**) along with the appearance of a new signal at δ 51.191 ppm which is due to the methoxy carbon (-O$\boldsymbol{C}$H$_3$) of FAME confirming the complete conversion of soybean oil to biodiesel. The olefinic protons (-C$\boldsymbol{H}$=C$\boldsymbol{H}$-) present in the carbon chain is indicated by the signal at δ 5.225–5.383 ppm in the oil (**Fig. 5.16**) and signal at δ 5.305–5.383 ppm in the biodiesel (**Fig. 5.17**). Accordingly, the olefinic carbons in the carbon chain of the oil and biodiesel showed signals at δ 127.824–130.022 ppm (**Fig. 5.18**) and δ 127.012–131.723 ppm (**Fig. 5.19**), respectively. The *bis*-allylic protons (-C=C-C$\boldsymbol{H}_2$-C=C-) of the unsaturated fatty acid chains are indicated by the ^{1}H NMR signal of oil at δ 2.749–2.780 ppm (t, ^3J = 6.2 Hz) and signal of FAME at δ 2.750–2.782 ppm (t, ^3J = 6.4 Hz). The signals at δ 2.290–2.323 ppm (t, ^3J = 6.4 Hz) in the ^{1}H NMR spectrum of oil and at δ 2.273–2.311 ppm (t, ^3J = 6.4 Hz) in the ^{1}H NMR spectrum of biodiesel are due to the α-methylene protons to the ester (-C$\boldsymbol{H}_2$-CO$_2$R) groups present in the oil and biodiesel, respectively. The signals due to α-methylene protons to the double bonds (-C$\boldsymbol{H}_2$-C=C-) of the carbon chains of the oil and biodiesel appeared at δ 2.001–2.071 ppm and δ 2.002–2.073 ppm, respectively. The β-methylene protons to the ester groups (-C$\boldsymbol{H}_2$-C-CO$_2$R) of the oil and biodiesel showed signals at δ 1.609 ppm and δ 1.600–1.634 ppm (t, ^3J = 6.8 Hz), respectively. The ^{1}H NMR signals of the methylene -(C$\boldsymbol{H}_2$)$_n$- protons of the fatty acid chain in the soybean oil and FAME are observed at δ 1.258–1.369 ppm and δ 1.286–1.371 ppm, respectively. The terminal methyl protons (-C$\boldsymbol{H}_3$) of the triglycerides and biodiesel are indicated by the ^{1}H NMR signals at δ 0.861–0.905 ppm and δ 0.862–0.907 ppm, respectively. The ^{13}C NMR signals at δ 172.596–173.016 ppm (**Fig. 5.18**) and δ 173.951 ppm (**Fig. 5.19**) are indicating the carbonyl carbons of the triglycerides and FAME, respectively. Accordingly, the ^{13}C NMR signals at δ 14.023–34.078 ppm in the triglycerides (**Fig. 5.18**) and at δ 13.958–33.928 ppm in the FAME (**Fig. 5.19**) are due to methylenes and methyl carbons of the long fatty acid chains.

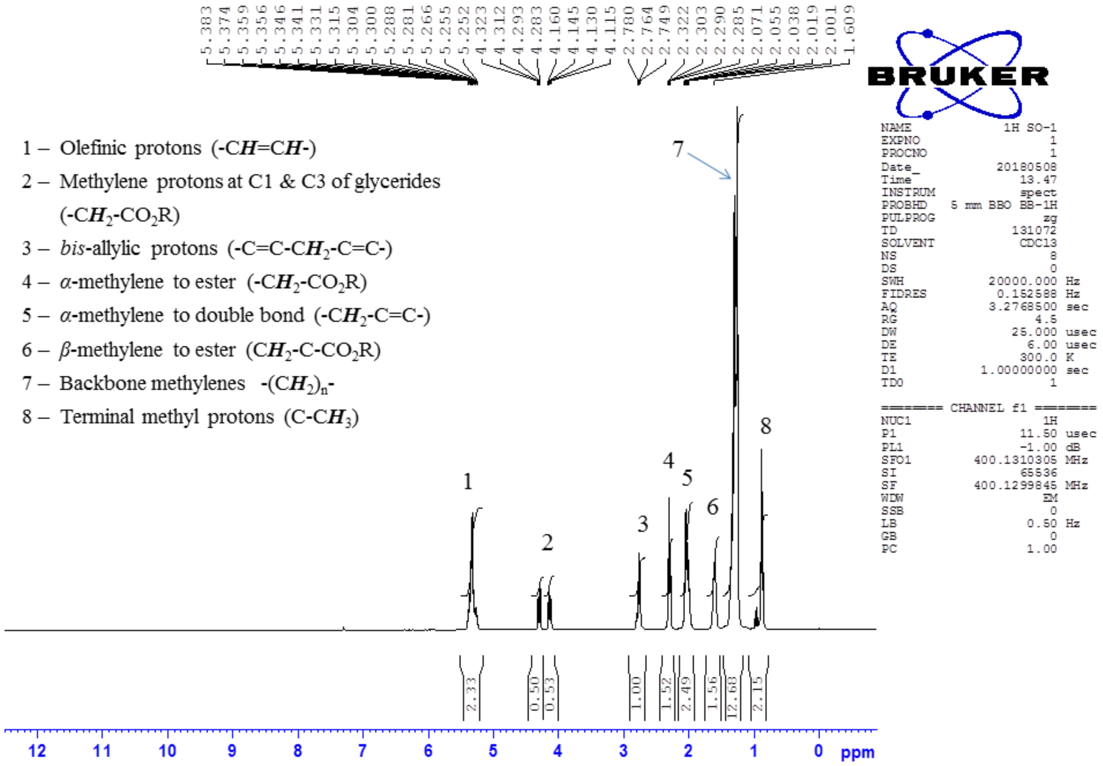

Fig. 5.16. ^{1}H NMR spectrum of soybean oil.

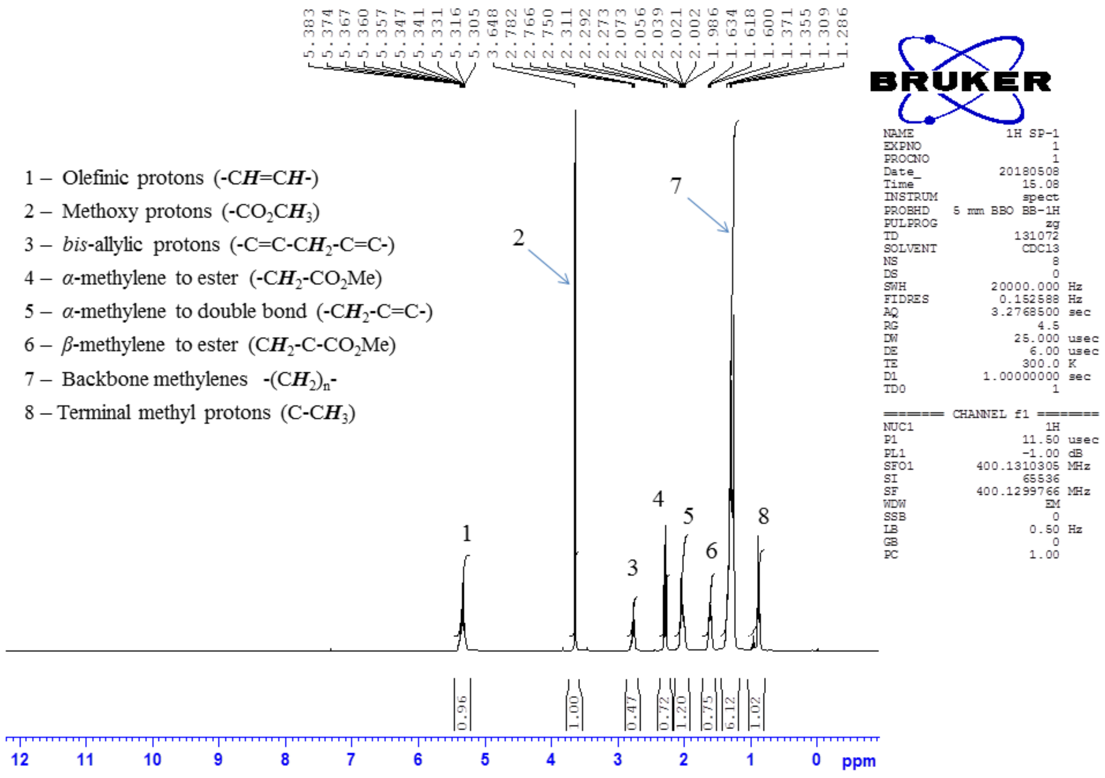

Fig. 5.17. ^{1}H NMR spectrum of biodiesel obtained from soybean oil.

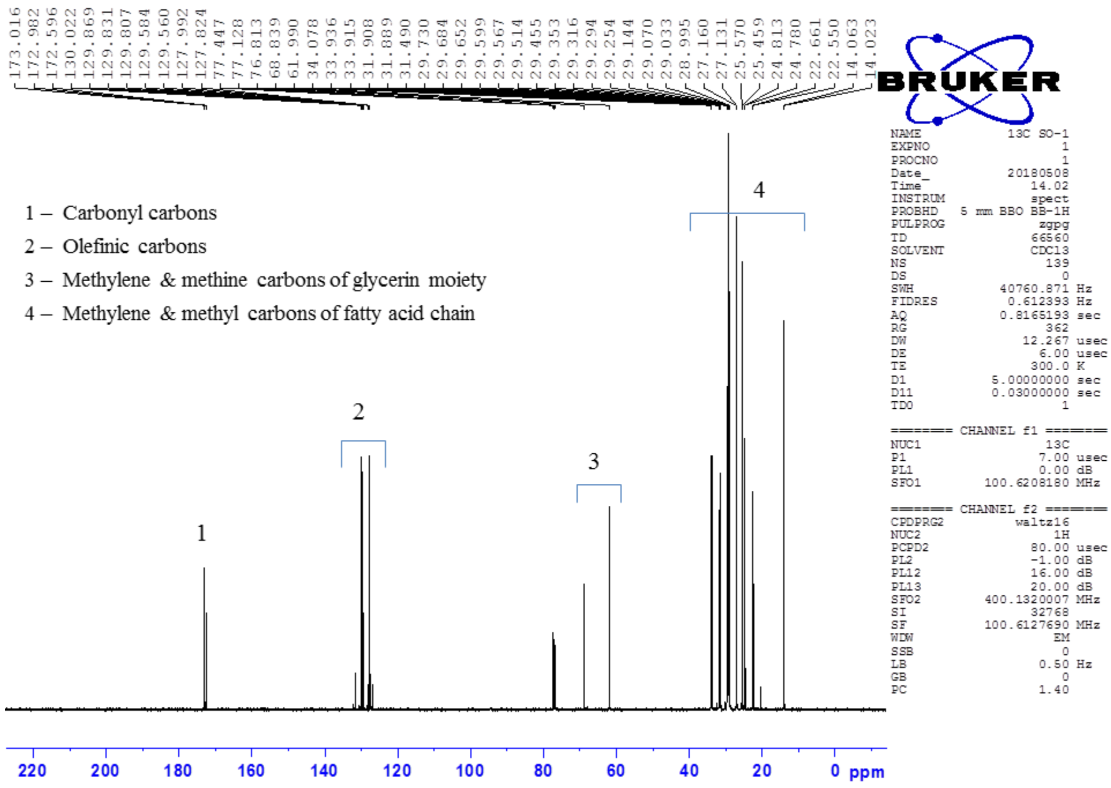

Fig. 5.18. ^{13}C NMR spectrum of soybean oil.

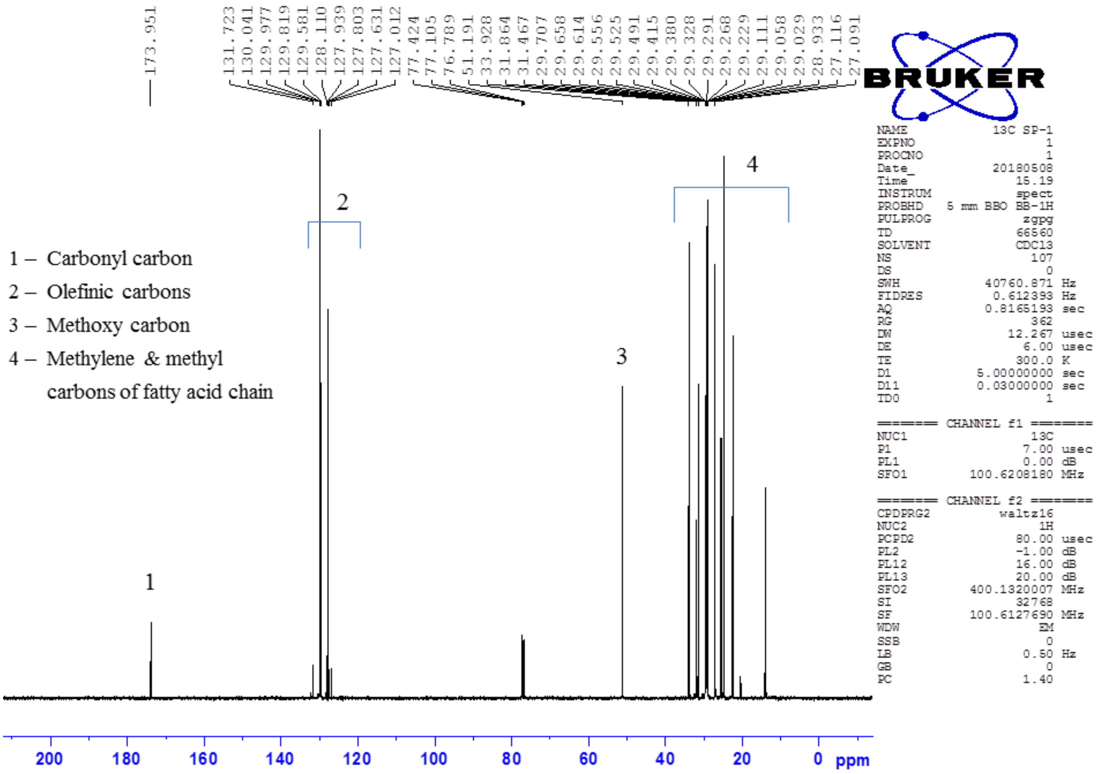

```
NAME                13C SP-1
EXPNO                      1
PROCNO                     1
Date_               20180508
Time                   15.19
INSTRUM                spect
PROBHD   5 mm BBO BB-1H
PULPROG                 zgpg
TD                     66560
SOLVENT                CDC13
NS                       107
DS                         0
SWH                40760.871 Hz
FIDRES              0.612393 Hz
AQ                 0.8165193 sec
RG                       362
DW                    12.267 usec
DE                      6.00 usec
TE                     300.0 K
D1                5.00000000 sec
D11               0.03000000 sec
TD0                        1

======= CHANNEL f1 ========
NUC1                     13C
P1                      7.00 usec
PL1                     0.00 dB
SFO1             100.6208180 MHz

======= CHANNEL f2 ========
CPDPRG2              waltz16
NUC2                      1H
PCPD2                  80.00 usec
PL2                    -1.00 dB
PL12                   16.00 dB
PL13                   20.00 dB
SFO2             400.1320007 MHz
SI                     32768
SF               100.6127690 MHz
WDW                       EM
SSB                        0
LB                      0.50 Hz
GB                         0
PC                      1.40
```

Fig. 5.19. ^{13}C NMR spectrum of biodiesel obtained from soybean oil.

5.3.6.3 GC-MS study

GC-MS was employed to identify the chemical composition of the FAMEs obtained from the transesterification of soybean oil. The library search reports (**Table 5.4**) of the GC peaks performed with TurboMass NIST 2008 (S/W) software reveal the presence of eight different methyl esters of fatty acids in the biodiesel. An unsaturated fatty acid ester *viz.* methyl linoleate (69.466%) was found to be the predominant FAME in the biodiesel followed by methyl palmitate (11.465%) which is a saturated fatty acid ester. Methyl myristate (0.224%), methyl stearate (3.503%), methyl gondoate (2.403%), methyl arachidate (1.849%), methyl behenate (2.874) and methyl lignocerate (0.858%) are the other fatty acid methyl esters which were detected in the biodiesel.

Table 5.4: GC-MS analysis of chemical composition of biodiesel

FAME	**Composition (%)**
Methyl myristate (C14:0)	0.224
Methyl palmitate (C16:0)	11.465
Methyl linoleate (C18:2)	69.466
Methyl stearate (C18:0)	3.503
Methyl gondoate (C20:1)	2.403
Methyl arachidate (C20:0)	1.849
Methyl behenate (C22:0)	2.874
Methyl lignocerate (C24:0)	0.858

5.3.6.4 Properties of soyabean oil biodiesel.

The fuel properties of soybean oil biodiesel were determined and compared with the standard limits prescribed by EN 14214 and ASTM D6751, and reported biodiesel properties (**Table 5.5**). The density of the soybean oil biodiesel at 15°C was found to be 0.8606 g cm^{-3} which is well within the range prescribed by EN 14214 as well as close to the reported values of other biodiesels (**Table 5.5**). The specific gravity of the biodiesel (0.8615) is in the agreement of the ASTM D6751 standard. The biodiesel with low viscosity is preferable for good combustibility as well as for non-deposition in the engine, and accordingly, the kinematic viscosity of the soybean oil biodiesel at 40°C was found to be low (3.76 mm^2 s^{-1}) which is well below the maximum limits of the standards. The kinematic viscosity found in the present study is comparatively lower than the previously reported values of biodiesel (**Table 5.5**)[11,105,106,111,114,115]. The cetane number of the produced biodiesel was 56.67 which is well above the minimum limit of international standards and close to the values reported by Deka and Basumatary [11] and Betiku et al. [105]. The calculated cetane index (56.13) of the biodiesel is also well comparable with the cetane number. The number of saponifiable units present per unit weight in the biodiesel indicated by saponification number (mg KOH/g) was found to be 176.33. The unsaturation in the biodiesel is determined by the iodine value and it was found to be 121.91 g I_2/100 g in the biodiesel of the present study which is very close to the maximum value prescribed by EN 14214. The pour point, cold filter plugging point and total sulphur of the biodiesel are found to be -3°C, 0°C and 2 ppm, respectively. The calculated diesel index, API value and aniline point of the biodiesel are found to be 55.309, 32.756 and 168.85, respectively. The higher heating value (HHV) of the biodiesel was determined and found to be 40.37 MJ/kg which is in well agreement with the reported values of 44.986, 39.25 and 43.19 MJ/kg [11,105,111].

Table 5.5: Comparison of properties of produced biodiesel with ASTM D6751, EN 14214 and reported biodiesel properties

Properties	**Soybean biodiesel (This work)**	**ASTM D6751**	**EN 14214**	**Reported biodiesel**					
				Thevetia peruviana [11]	**Jatropha** [111]	***Bauhinia monandra*** [105]	**Palm** [106]	**Jatropha** [114]	***Azadirachta indica*** [115]
Density (15°C, g/cm^3)	0.8606	NS	0.86–0.90	0.875	0.875	0.876	0.86	0.891	0.887
Specific gravity	0.8615	0.86–0.90	0.85	–	0.875	0.876	0.86	0.892	0.887
Kinematic viscosity (40°C, mm^2/s)	3.76	1.9–6.0	3.5–5.0	4.33	5.7	4.90	4.3	6.8	5.3
Cetane number	56.67	47 (min)	51 (min)	61.5	48.6	59.83	76.93	–	83
Cetane index	56.13	NS	NS	62.9	–	–	–	–	–
Pour point (°C)	-3	NS	NS	+3	3	0	-6	–	-10
CFPP (°C)	0	NS	NS	–	–	–	–	–	–
Saponification number (mg KOH/g)	176.33	NS	NS	–	–	–	–	–	–
Iodine value (g I_2/100 g)	121.91	NS	120 (max)	69.9	119	52.22	40.90	–	58.96
API	32.756	36.95	NS	–	0.875	30.03	32.42	0.892	28.20
Diesel index	55.309	50.4	NS	–	–	69.21	92.95	–	102.36
Aniline point	168.85	331	–	–	–		–	–	358
Total sulphur (ppm)	2	15 (max)	10 (max)	–	–	–	–	–	–
HHV (MJ/kg)	40.37	NS	NS	44.986	39.25	43.19	–	37.100	45.88

NS–Not specified; CFPP–Cold filter plugging point; API–American petroleum index; HHV–Higher heating value.

5.4 Conclusion

In this work, we have explored easily available agro-waste plant derived *B. nigra* ash as a highly efficient, renewable and recyclable heterogeneous catalyst for biodiesel production from both edible and non-edible oils. The thorough characterization of ash catalyst confirmed the polycrystallinity and microporosity of the materials. The presence of higher quantity of K revealed from AAS (343.89 ppm), EDX (56.13%) and XPS (15.13%) in the form of carbonate and oxide indicated by XRD played the key role for the transesterification of oil into biodiesel. The catalyst showed high yield (98.79%) of biodiesel from soybean oil in a short time period of 25 min at 65^{o}C under the ORCs. The study exhibited similar catalytic activity for biodiesel synthesis from both edible and non-edible oils (Jatropha oil and *Thevetia peruviana* oil) under the identical reaction conditions. The simplicity and easier of the reaction are supported with low activation energy (27.87 kJ mol^{-1}). The catalyst was reused up to the 3rd cycle of reaction that yielded 96% biodiesel without significant loss in the catalytic activity. Thus, utilization of waste *B. nigra* plant will provide the low-cost catalyst preparation, reaction simplicity, no disposal problems, waste to wealth management and green expertise with effective catalytic activity for biodiesel synthesis at large scale. In addition, it will help to reduce biodiesel cost as well as greenhouse gas emission in the environment.